Available online at www.sciencedirect.com
ScienceDirect
Journal of Catalysis 243 (2006) 376–388
JOURNAL OF CATALYSIS
www.elsevier.com/locate/jcat

Selective production of methoxyphenols from dihydroxybenzenes on alkali metal ion-loaded MgO

Munusamy Vijayaraj, Chinnakonda S. Gopinath *

Catalysis Division, National Chemical Laboratory, Dr. Homi Bhabha Road, Pune 411 008, India

Received 2 August 2006; accepted 15 August 2006

Abstract

Selective O-methylation of dihydroxybenzenes (DHBs; catechol, resorcinol, and hydroquinone) to methoxyphenols (MPs) was carried out with dimethylcarbonate on MgO and alkali metal ion (Li, K, and Cs)-loaded MgO between 523 and 603 K. Catalytic activity and product selectivity varied with respect to DHB substrates. Selectivity for O-methylated products increased with increasing basicity of alkali ions; however, K-MgO showed high and stable activity toward MPs. Selectivity for MPs obtained from three substrates increased in the following order: catechol < resorcinol < hydroquinone. The mode of interaction of substrates on the catalysts surface influenced reactivity and product selectivity. It is likely that the low reaction temperatures used (<603 K) kinetically control and favor high MP selectivity from DHBs. Calcined and spent catalysts were characterized by XRD, surface area, SEM, thermal analysis, NMR, and XPS. XRD analysis revealed the formation of alkali oxide phases on alkali-loaded MgO. Crystallite size and surface area of the catalysts decreased after methylation reactions, except on K-MgO. TGA showed 40–60 wt% coke deposition on spent catalysts. TGA in N_2 followed by air and ^{13}C CP-MAS NMR measurements indicated the nature of deposited carbon to be molecular species, graphite, $MgCO_3$ and polyaromatics. XPS revealed the nature and availability of active sites on the spent catalysts, as well as the same changes with reaction conditions and correlated with catalytic activity.

Keywords: MgO; K-MgO; Alkali-loaded MgO; Dihydroxybenzene; Methoxyphenol; XPS; O-methylation; Thermal analysis

1. Introduction

Innovations in solid catalysts for the production of fine chemicals and bulk chemicals have lead researchers to attempt vapor-phase methylation (or alkylation) of phenols with dimethylcarbonate (DMC), methanol (or alcohols) over metal oxides [1–23], sulfates [24,25], phosphates [26], and zeolites [27–29]. O-methylated dihydroxybenzenes (DHBs) and phenols are widely used in the production of variety of fine chemicals and valuable synthetic intermediates [30]. For instance, 2-methoxyphenol (2-MP), derived from O-methylation of catechol, is an important precursor in the preparation of vanillin. Similarly, 3-methoxyphenol (3-MP) and 4-methoxyphenol (4-MP) are used as UV inhibitors, antioxidants for oil and grease, and polymerization inhibitors. Selective catalytic production of methoxyphenols (MPs) from DHBs is an interesting and challenging problem from both process and kinetic control standpoints. However, few reports are available in the literature [31–46].

Ono et al. [31–34] reported the selective O-methylation of catechol over alkali hydroxide/nitrate-loaded alumina. DMC was found to be a more efficient methylating agent than methanol over alumina. The main product obtained was 2-MP, with 70% selectivity at 583 K. Over K/Al_2O_3, a high 1,2-dimethoxybenzene (1,2-DMB) yield of 97% was obtained at 583 K with DMC:catechol = 4. Li/Al_2O_3 was found to be a selective catalyst for the 2-MP formation (84%) with 100% catechol conversion at 583 K. On Cs/Al_2O_3, catechol methylation yielded 2-MP and catechol carbonate (PCC), which further reacted with DMC, resulting in 1,2-DMB formation.

Cavani et al. [35–37] found boron phosphate (BPO_4) to be an efficient catalyst for the monoetherification of catechol, aimed at the production of 2-MP. BPO_4 catalyst with B/P = 1 displayed best results in terms of catechol conversion, 2-MP se-

* Corresponding author. Fax: +91 20 2590 2633.
E-mail address: cs.gopinath@ncl.res.in (C.S. Gopinath).

0021-9517/$ – see front matter
doi:10.1016/j.jcat.2006.08.009

lectivity, and stability with TOS at 548 K. The optimal surface acidity and low temperature made the undesired reactions of tar formation and ring methylation much slower. However, this catalyst on alumina support had a lower activity than BPO_4. Vishwanathan et al. [38] reported the vapor-phase methylation of catechol over solid base catalysts, like Cs-loaded TiO_2, Al_2O_3, and SiO_2 at 623 K. Good selectivity to 2-MP was achieved, and TPD studies indicated the presence of weak basic sites and their participation in the O-methylation process. Rao et al. [39,40] found that using Mg–Al hydrotalcite as a catalyst for the synthesis of 2-MP gave an 80% yield at 573 K. A concerted mechanism was proposed involving acid–base pair sites with nucleophilic attack at the methyl carbon atom of DMC by the phenolic oxygen or phenolate anion.

Renken et al. [41,42] studied regulation to control the selectivity in vapor-phase methylation of catechol to 2-MP over modified alumina at 598 K. A 20-fold change in the O/C-methylation ratio was achieved by varying the catalyst acid–base properties. Catalytic activity and selectivity toward 2-MP formation was found to increase with surface acidity. Sivasanker et al. [43,44] reported O-methylation of DHB on alkali metal ion-loaded silica at relatively high temperature (673 K). Catalyst activity and selectivity for DMB increased with metal loading and basicity of the metal ions. The order of reactivity of the three DHBs increased in the following order: catechol < hydroquinone < resorcinol. Assuming the methylation process as pseudo-first-order kinetics, the ratio of rate constants of second methylation to first methylation (K_2/K_1) was found to predict the ratio of DMB to total methoxy products [44]. Recently, Zhu et al. [45] reported 2-MP production from Ti containing $AlPO_4$ at 553 K. In another report, Fu et al. [46] explored $ZnCl_2$-modified Al_2O_3 for O-methylation of catechol with MeOH at 553 K. A weak coordination of catechol with Zn^{2+} sites led to 82% 2-MP selectivity. $ZnCl_2$ leaching and surface coking during the reaction run were the main causes of catalyst deactivation. It is clear from the literature reports that the alkali metal ions enhance the basicity of the catalyst [47,48], which in turn improves the O-methylation activity.

Although O-methylation for catechol has been evaluated, that of resorcinol and hydroquinone has not been measured in detail [43,44]. We have attempted O-methylation of all three DHBs with DMC on MgO and alkali ion (Li, K, and Cs)-loaded MgO to selectively produce MPs. The high and stable activity observed on K-MgO indicates an optimum basicity required for O-methylation. X-ray diffraction (XRD), surface area, NMR, photoemission and thermal analysis on calcined and spent catalysts reveal the mechanisms behind catalyst deactivation. A plausible methylation mechanism is suggested from the reaction and spent catalyst characterization results.

2. Experimental

2.1. Catalyst preparation and methylation

Magnesium oxide light (Merck, India) was used as a catalyst/support. Alkali metal ions (Li, K, and Cs) were loaded onto the MgO by an impregnation method using an aqueous solution of $LiOH{\cdot}H_2O$, KNO_3, and $CsNO_3$ at 353 K. The as-synthesized catalysts were dried at 383 K for 12 h, pelletized, and sieved to a mesh size of 25–30. An identical but blank wet impregnation was carried out with MgO, and the resulting $Mg(OH)_2$ was used after activation as pure MgO catalyst. The catalytic measurements were carried out in vertical downflow glass reactor (18 mm i.d.) with 0.5 g of sieved catalyst packed between inert porcelain beads and placed inside a vertical furnace (Geomechanique, France) [49,50]. The catalyst was activated in situ with a stream of air at 673 K for 2 h for nitrate and hydroxide decomposition, then flushed with stream of N_2 (10 mL/min) while bringing down to the desired reaction temperature. Note that the above in situ activation decreases the weight of the loaded catalyst due to the decomposition of nitrate/hydroxide, and the exact weight was obtained by simulating the same in thermogravimetric analysis (TGA) and used for space velocity calculations. The feed mixture (DMC + DHB) was passed into the reactor using a syringe pump in a N_2 stream (10 mL/min). Products were identified by gas chromatography–mass spectrometry (GC–MS), using a Schimadzu GC-17A equipped with a QP 5000 mass spectrometer, and analyzed by GC, using an Agilent 6890 J-413 with an HP-5.5% phenyl methyl siloxane capillary column equipped with a flame ionization detector.

2.2. Catalyst characterization

XRD patterns of the powder samples were recorded with a Rigaku Geigerflex instrument using Cu$K\alpha$ radiation (1.5405 Å) with a Ni filter to identify the different phases. The crystallite size of the catalysts was calculated using Scherrer's equation [51]. The BET surface area and the pore volume (V_p) of the catalysts were determined by N_2 adsorption–desorption method at 77 K using a Quanta chrome NOVA-1200 adsorption unit. Activated catalysts were subjected to energy-dispersive X-ray (EDX) analysis for bulk composition; the results were within the expected range. Thermal analysis was measured by a Perkin–Elmer Diamond TG/DTA with Al_2O_3 as the internal standard. About 10 mg of the spent K-MgO catalyst was taken after methylation testing with any DHB for 1 h and was subjected to temperature ramping up to 1500 K in the flow of air or N_2 (100 mL/min) at a heating rate of 10 K/min. ^{13}C cross-polarization magic-angle spinning (CP-MAS) NMR measurements were carried out with an MSL Bruker spectrometer operating at 75.15 MHz on solid spent catalysts from catechol and resorcinol methylation after 1 h TOS. X-ray photoelectron spectra (XPS) were acquired from a VG Microtech Multilab ESCALAB 3000 spectrometer using a nonmonochromatized Mg$K\alpha$ X-ray source (1253.6 eV) [49,50]. Base pressure in the analysis chamber was maintained in the range of 3–6 $\times$ 10^{-10} Torr. Energy resolution of the spectrometer was set at 0.8 eV with Mg$K\alpha$ radiation at a pass energy of 20 eV. The error in the reported binding energy (BE) values is $\pm$0.1 eV.

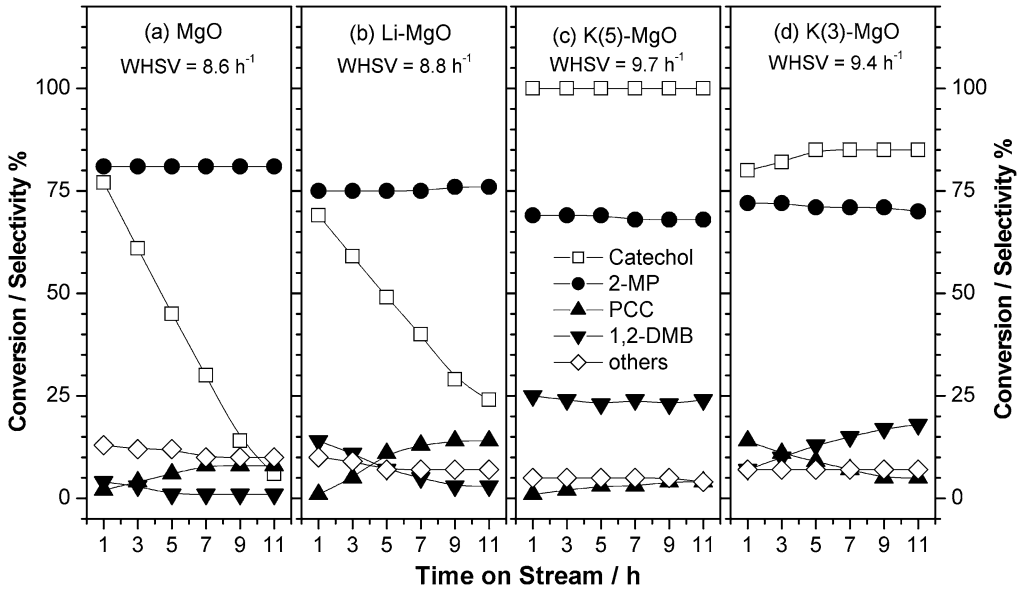

Fig. 1. Selective O-methylation of catechol to 2-methylphenol at 583 K on MgO and 5 mmol alkali ion-loaded MgO, with DMC:catechol = 2:1 feed mixture. Alkali ion content loaded on MgO in mmol is given in parentheses. Catechol methylation on 3 mmol K-loaded MgO at 583 K also shown to show the dependence on alkali loading.

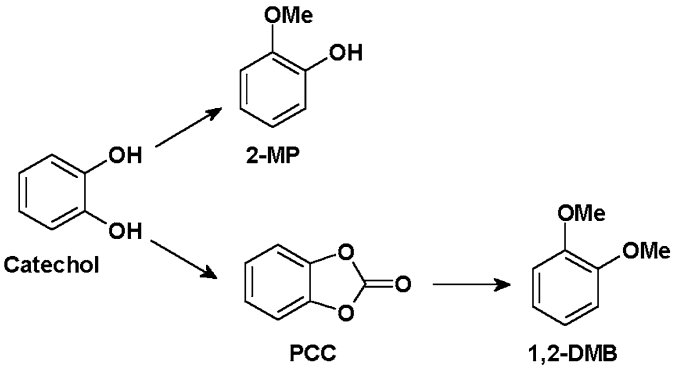

Scheme 1. Catechol methylation with DMC (DMC:catechol = 2) on MgO and alkali ion-loaded MgO. Highly selective (97%) production of 1,2-DMB with DMC:catechol = 4 hints a direct methylation.

3. Results

3.1. Catechol methylation

Fig. 1 shows catechol conversion and 2-MP selectivity on pure MgO and Li- and K-loaded MgO with DMC at 583 K. The amount of alkali metal nitrate/hydroxide loaded was 5 mmol per gram of MgO. Reaction results from 3 mmol KNO_3-loaded MgO are also shown in Fig. 1. Li- and Cs-loaded MgO showed very similar results, and hence the latter results are not shown. 2-MP formed as a major product along with PCC, 1,2-DMB, and C-methylated products (3-methylcatechol, 3-methylguaiacol, and 4-methylguaiacol), as indicated in Scheme 1. The 5 mmol K^+-loaded MgO (K-MgO) showed stable and 100% catechol conversion; however, on all other systems, the conversion decreased continuously. The 3 mmol (and 1 mmol) K^+-loaded MgO showed lower conversion for all three DHBs, with the extent of O-methylation decreasing with a decreasing amount of K^+ ions. All further studies were carried out exclusively on 5 mmol-loaded systems. In fact, the stable activity on K-MgO clearly indicates that the genesis of activity was due mostly to potassium and the associated overall intermediate basicity on K-MgO. The decreased catechol conversion on MgO and Li/Cs-MgO suggests that a low or high basicity did not assist the reaction. Indeed, a similar trend was observed with other substrates, like resorcinol and hydroquinone, and the same explanation holds.

On MgO (Fig. 1a), 2-MP selectivity was 80% and C-methylated products formed dominantly over 1,2-DMB and catechol carbonate (PCC). However, with Li (K) loading on MgO, 2-MP selectivity decreased marginally to 75% (70%) and C-methylated product selectivity dropped to 5% on K-MgO (Figs. 1b and 1c). 1,2-DMB (PCC) formation decreased (increased) with TOS on MgO as well as on Li-MgO. In contrast, the sizeable amount of 1,2-DMB formed (24%) on K-MgO indicates a higher O-methylation capacity compared with the other systems. Suppression of PCC formation at the cost of 1,2-DMB on K-MgO was noted and compared with that on Li- or Cs-MgO catalysts.

Feed composition studies on K-MgO at 573 K with DMC:catechol = 2 and 4 are shown in Fig. 2. Needless to say that 100% catechol conversion was obtained in both cases; however, product selectivity changed dramatically with the amount of DMC. An abrupt change occurred in 1,2-DMB selectivity (from 24 to 97%) for a change in the DMC:catechol ratio from 2 to 4. Only trace amounts of 2-MP and C-methylated products and no PCC were formed at a feed ratio of 4. Fig. 2 also shows DMC conversion with respect to TOS, indicating that 60–65% DMC reacted for the complete conversion of catechol to methylated products, and hence effective utilization occurred.

The effect of reaction temperature (523–583 K) was evaluated on K-MgO with DMC:catechol = 2 (Fig. 3). Catechol conversion increased from 25% at 523 K to nearly 100% at

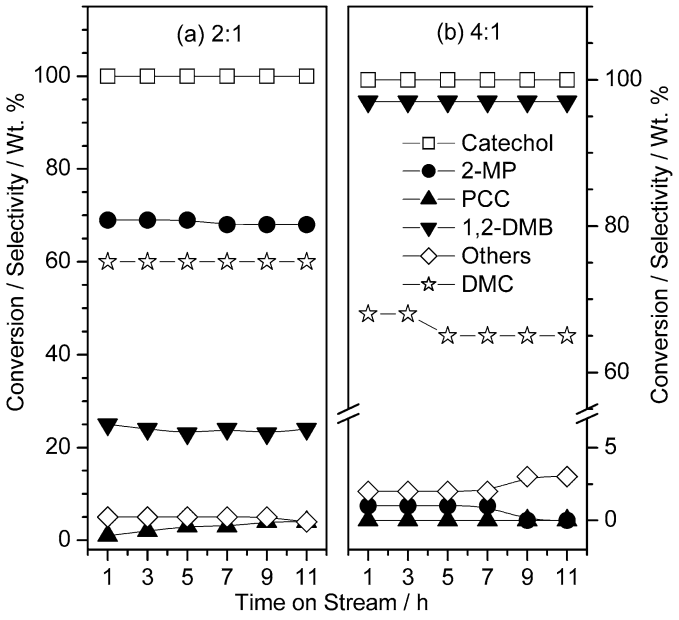

Fig. 2. Feed composition dependence of O-methylation catalytic activity and products selectivity on K(5)-MgO at 583 K at WHSV = 9.7 h^{-1}.

553 K and then reached 100% at 583 K. 2-MP selectivity was marginally affected at 523 K and remained at around 70% between 553 and 583 K. Note that PCC formation increased with TOS (18–36%) at 523 K. 1,2-DMB (PCC) selectivity increased (decreased) with increasing temperature from 523 to 583 K. This indicates that 1,2-DMB formed at the expense of PCC at high reaction temperature and that this formation was not likely through subsequent methylation of 2-MP.

Weight hour space velocity (WHSV)-dependent studies were carried out on K-MgO with a DMC:catechol = 2 feed at 583 K (Fig. 4). The results clearly indicate that catechol conver-

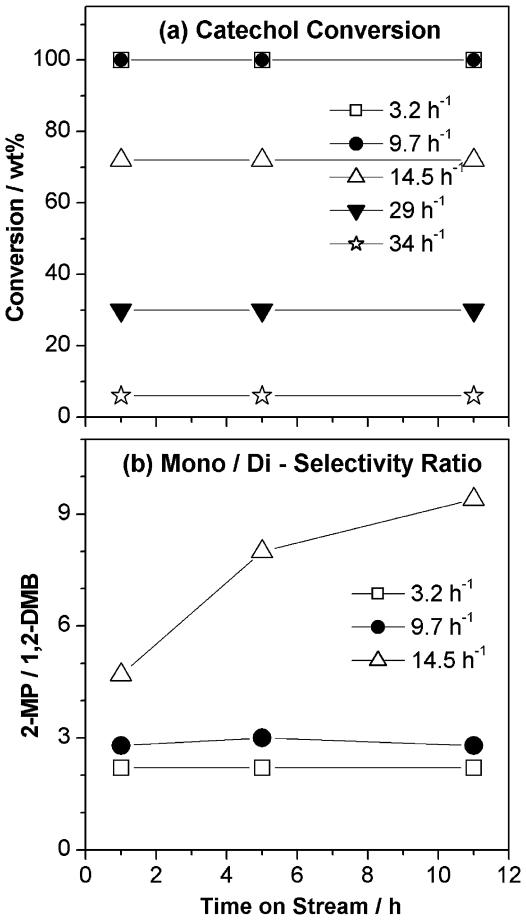

Fig. 4. Space velocity dependence of (a) catechol conversion and (b) the ratio between 2-methylphenol to 1,2-dimethoxybenzene (mono to di methylation) at 583 K on K(5)-MgO with DMC:catechol = 2:1 feed mixture. It is to be noted that at high WHSV, 2-MP was produced exclusively and hence 2-MP to 1,2-DMB ratio is not given in panel (b).

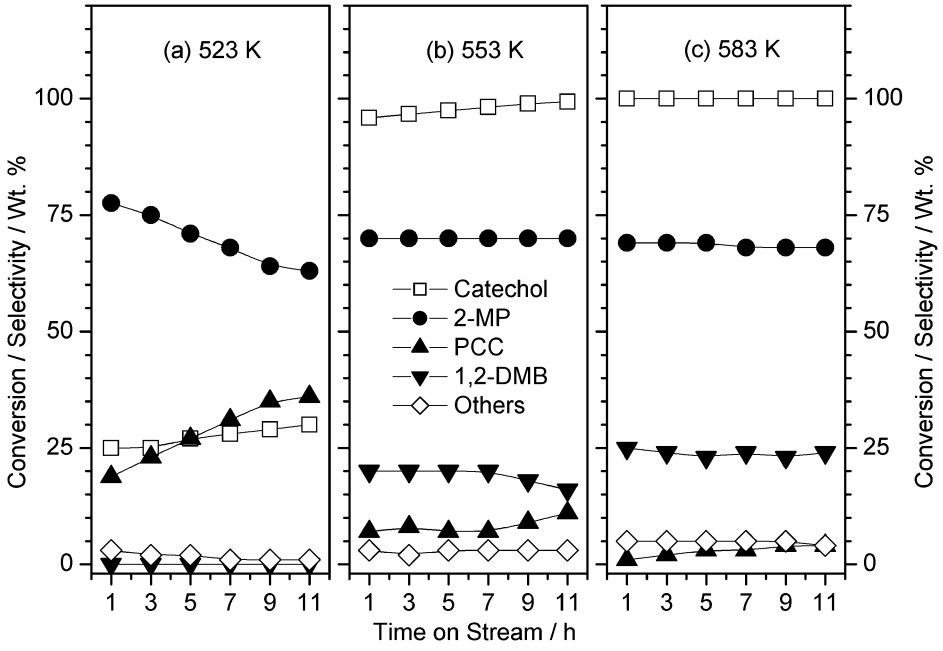

Fig. 3. Reaction temperature dependence of catechol conversion and products selectivity on K(5)-MgO at a WHSV = 9.7 h^{-1} with DMC:catechol = 2:1 feed mixture.

sion was significantly affected by changes in WHSV. Although catechol conversion decreased to 1/3 by increasing the space velocity from 9.7 to 29 h^{-1}, the initial conversion level for any WHSV value remained at the same level for up to 12 h, indicating stable catalytic activity (Fig. 4a). Fig. 4b expresses 2-MP selectivity in terms of the 2-MP to 1,2-DMB (mono to di) ratio, showing a ratio of >1, indicating the selective monomethylation over dimethylation. The above methylation ratio increased exponentially at higher space velocity, and 2-MP selectivity increased to 100% with no C-methylated products at a space velocity >14.5 h^{-1}.

3.2. Resorcinol methylation

Table 1 shows resorcinol methylation activity and product selectivity on MgO and alkali metal ion-loaded MgO. 3-MP formed as a major product with 1,3-DMB (Scheme 2) and other C-methylated products (4-methylresorcinol, 6-methyl-3-guaiacol, and 4-methyl-3-guaiacol) as side products on all of the catalysts. A high initial resorcinol conversion (>65%) at TOS = 1 h was observed in the TOS-dependent studies, indicating the possibly high potential of all catalysts. K-MgO showed 80–90% conversion up to TOS = 3 h. Nonetheless, the conversion decreased from the initial levels to about ⩽40% (⩽15%) on Li- and K-MgO (MgO and Cs-MgO) catalysts. Some high boiling biphenolic molecular fragments were also identified from reaction products by GC-MS. 3-MP selectivity remained high (>70%) on all of the catalyst systems independent of TOS. Cs-MgO showed faster deactivation than MgO even though the highest 3-MP selectivity (>90%) was observed. Significant aromatic ring methylation was observed on all systems except Cs-MgO.

Table 1
Comparison of O-methylation activity of resorcinol with DMC:resorcinol = 2:1 feed mixture at 583 K and TOS = 3 h

Catalysts (WHSV in h^{-1})	Conversion (wt%)	Products selectivity (%)		
		3-MP	1,3-DMB	Others
MgO (8.6)	28	79.7	3.5	16.8
Li-MgO (8.8)	43.6	69	4.5	26.5
K-MgO (9.7)	81.6	83	11	6
Cs-MgO (8.6)	21.2	94	3	3

Fig. 5 shows a systematic increase in resorcinol conversion with increasing temperature from 543 K on K-MgO; however, deactivation was also observed with increasing TOS at all temperatures studied. At lower temperatures (543 and 563 K), 3-MP formed selectively (90–97%) with traces of C-methylated resorcinol and 1,3-DMB. Secondary products formed appreciably at 583 K and above at the expense of 3-MP. 1,3-DMB formed in the initial few hours of reaction at 583 K and above at the expense of 3-MP, indicating the stepwise methylation of 3-MP to 1,3-DMB.

Fig. 6 shows the effect of the DMC:resorcinol molar ratio on reactant conversion and product selectivity on K-MgO. It is very interesting to note that the catalyst deactivation rate decreased with increasing DMC:resorcinol ratio from 2 to 4. A stable resorcinol conversion was observed for at least up to

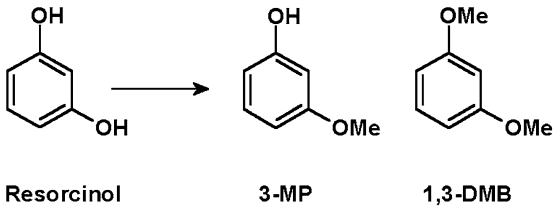

Scheme 2. Resorcinol methylation with DMC on MgO and alkali ion-loaded MgO. Ratio of 3-MP/1,3-DMB varies with the ratio of DMC:resorcinol as well as time on stream.

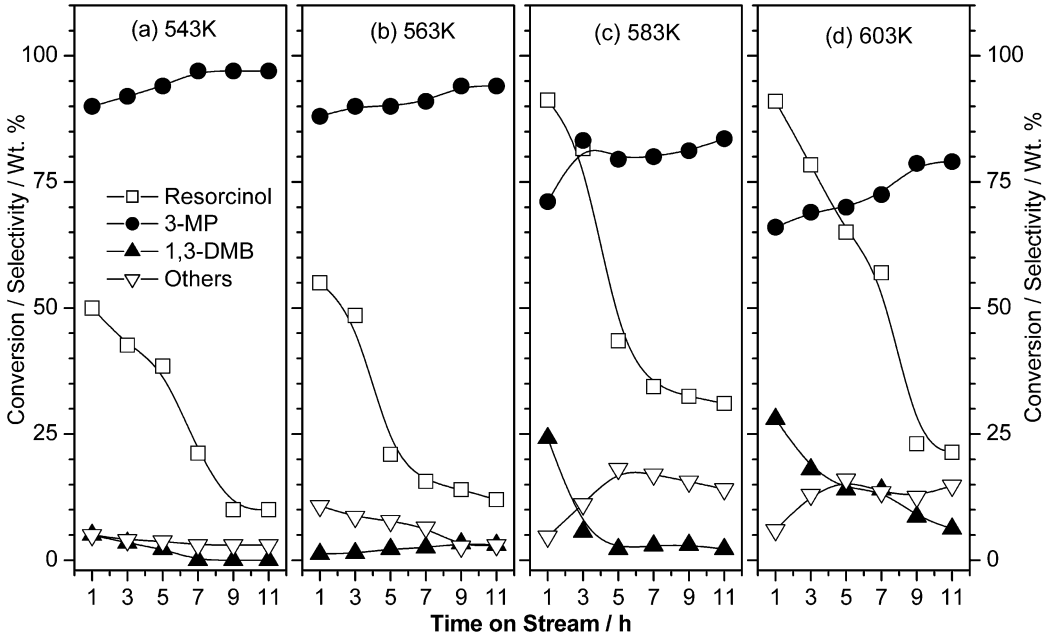

Fig. 5. Reaction temperature dependence of resorcinol conversion and products selectivity on K(5)-MgO at WHSV = 9.7 h^{-1} with DMC:resorcinol = 2:1 feed mixture.

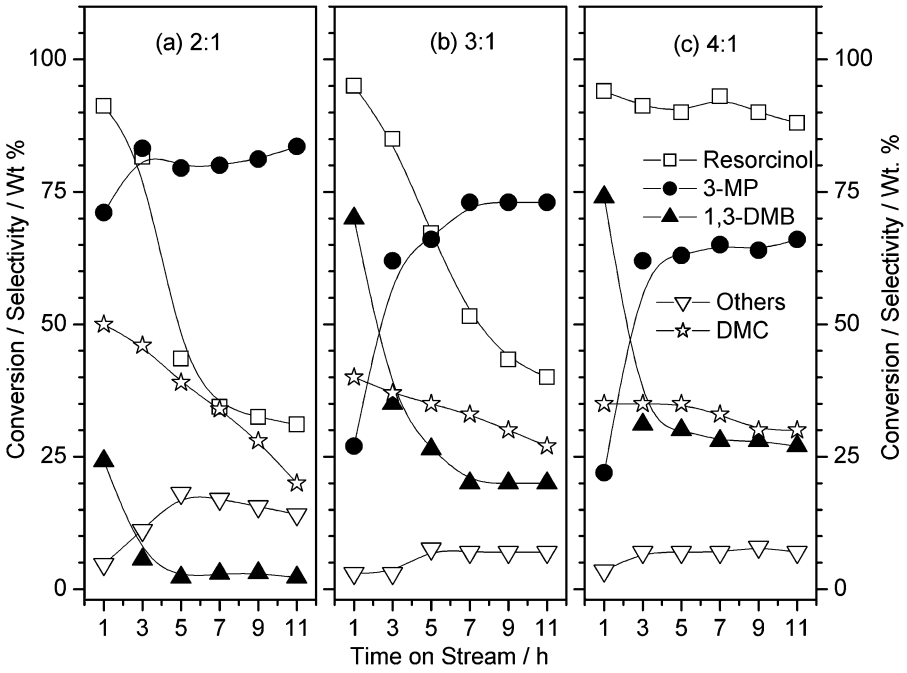

Fig. 6. Feed composition (DMC:resorcinol) dependence of O-methylation catalytic activity and products selectivity on K(5)-MgO at 583 K and at WHSV = 9.7 h^{-1}.

11 h for a DMC:resorcinol ratio of 4 (Fig. 6c). 3-MP (1,3-DMB) selectivity increased (decreased) after the transient state at a TOS of ca. 1 h. The above results clearly demonstrate that excess DMC hindered the catalyst deactivation. Recyclability of K-MgO was tested after the reactions shown in Figs. 6a and 6b. There was a considerable decline of 5% conversion on every recycling after complete carbon burning; however, the selectivity remained the same.

Fig. 7 shows the effect of space velocity on resorcinol conversion and 3-MP/1,3-DMB (mono to di) selectivity ratio at various TOS on K-MgO with DMC:resorcinol = 4 at 583 K. A stable resorcinol conversion was observed for all space velocities used, although conversion decreased with increasing space velocity (Fig. 7a). O-methylation activity plotted in terms of mono to di ratio was >1 at WHSV > 14.5 h^{-1}. This indicates a high 3-MP selectivity is possible by reducing the substrate–catalyst contact time. Also note that with increasing TOS, the mono/di ratio increased substantially at all WHSVs.

3.3. Hydroquinone methylation

Hydroquinone methylation on MgO- and alkali ion-loaded MgO with a DMC:hydroquinone = 2 feed ratio at 583 K was carried out; the results are given in Table 2. Methanol was added in the feed as solvent for all hydroquinone methylation studies, because it is sparingly soluble in DMC. As such, methanol had no methylation activity on these catalysts. This was confirmed by experiments with methanol and hydroquinone that showed no methylation. 4-MP formed selectively along with small amounts of 1,4-DMB and 2-methylhydroquinone (Scheme 3). MgO, Li, and Cs-MgO showed ca. 30% initial conversion (from TOS-dependent studies; not shown) with >85% 4-MP selectivity. Nevertheless, K-MgO showed stable hydroquinone conversion (80%) and selectively produced 4-MP (95%). Gener-

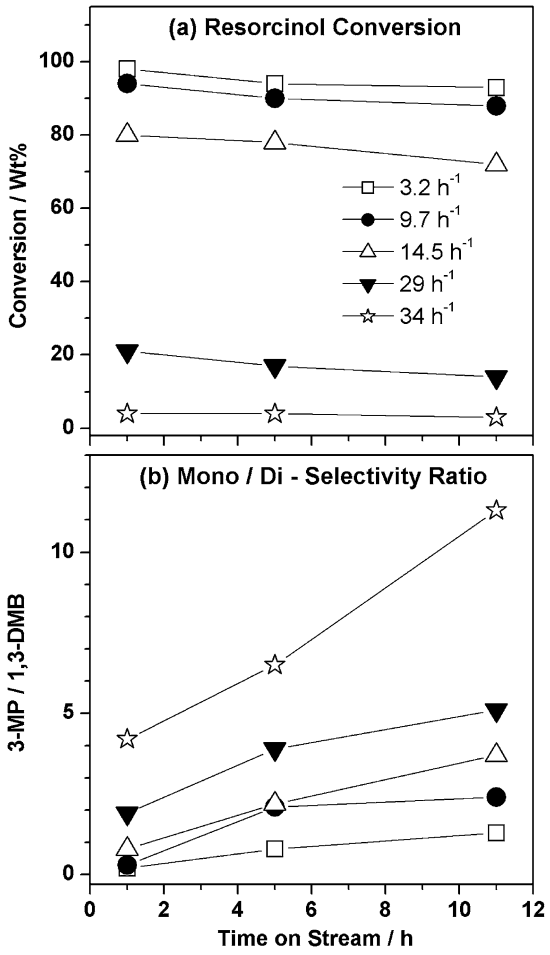

Fig. 7. Space velocity dependence of (a) resorcinol conversion and (b) the ratio between 3-methoxyphenol to 1,3-dimethoxybenzene (mono to di methylation) at 583 K on K(5)-MgO with DMC:resorcinol = 4:1 feed mixture.

Table 2
Comparison of O-methylation activity of hydroquinone with DMC:hydroquinone = 2:1 feed mixture at 583 K and TOS = 3 h

Catalysts (WHSV in h^{-1})	Conversion (wt%)	Product selectivity (%)		
		4-MP	1,4-DMB	Others[a]
MgO (8.6)	24	85	1	14
Li-MgO (8.8)	28	90	1	9
K-MgO (9.7)	83	94	4	2
Cs-MgO (8.6)	10	98	2	0

[a] Mainly consisting 2-methylhydroquinone.

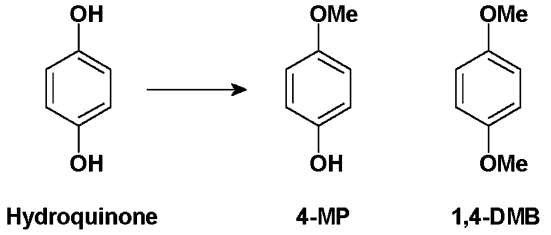

Scheme 3. Hydroquinone methylation with DMC on MgO and alkali ion-loaded MgO catalysts.

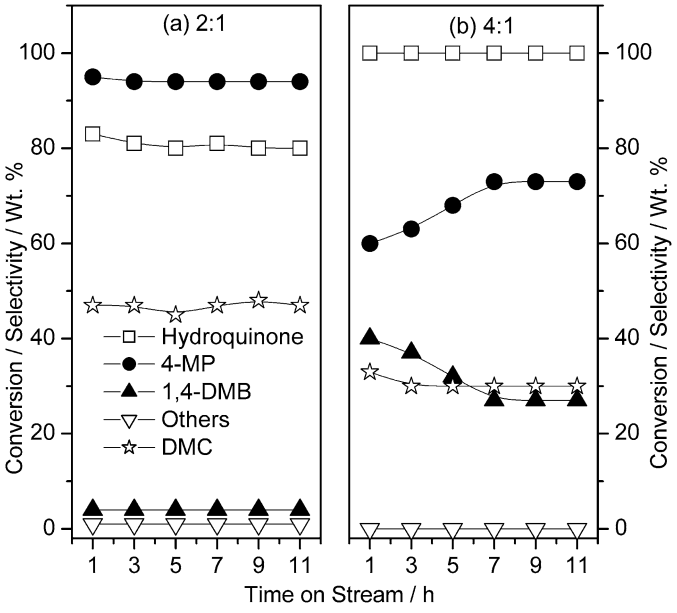

Fig. 8. Feed composition (DMC:hydroquinone) dependence of hydroquinone and DMC conversion and products selectivity on K(5)-MgO at 583 K and at WHSV = 9.7 h^{-1}.

ally, selectivity for 4-MP increased considerably on alkali ion-loaded MgO.

Fig. 8 shows the feed composition dependence with DMC: hydroquinone molar ratios of 2 and 4 on K-MgO at 583 K. At a DMC:hydroquinone ratio of 2, 80% hydroquinone conversion with 95% selectivity for 4-MP was found (Fig. 8a). At a molar ratio of 4, 100% hydroquinone conversion was observed; however, selectivity for 4-MP dropped to 70% with an increase in 1,4-DMB formation (30%). Higher DMC content in the feed led to O-methylation of both OH groups. The DMC conversion was 50% at a DMC:hydroquinone ratio of 2 and 30% at a ratio of 4, indicating a significant loss of DMC in side reactions like gasification, dissociation, and others.

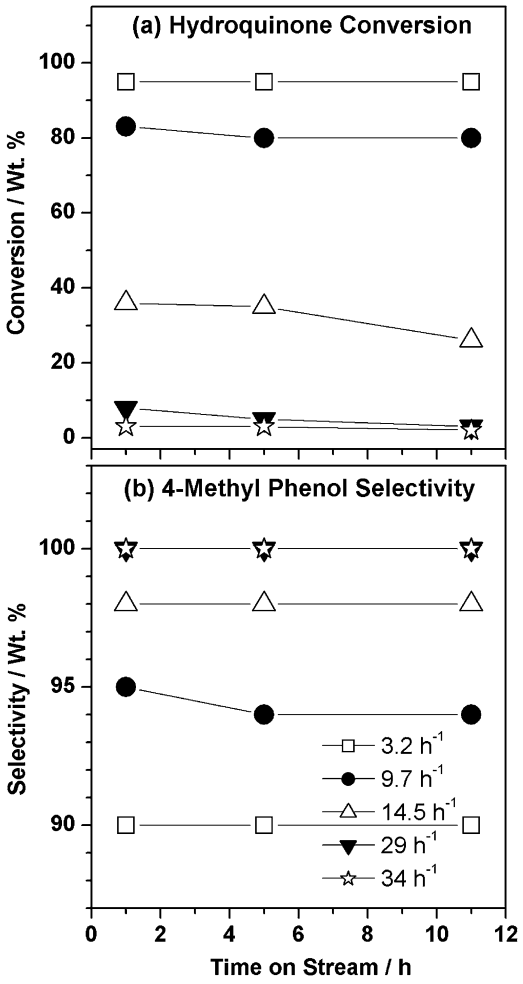

Fig. 9. Space velocity dependence of hydroquinone conversion and 4-methoxy phenol selectivity at 583 K on K(5)-MgO with DMC:hydroquinone = 2:1 feed mixture.

Space velocity influenced hydroquinone conversion and 4-MP selectivity, as shown in Fig. 9. Reaction was measured on K-MgO with DMC:hydroquinone = 2. Hydroquinone conversion decreased rapidly from 95 to 3% with increased space velocity from 3.2 to 34 h^{-1}. 4-MP was produced with 90–100% selectivity at all space velocities used.

3.4. Textural properties of activated and spent catalysts

The powder XRD patterns from calcined catalysts are shown in Fig. 10a. It is evident that the single phase of MgO periclase (ASTM 4-0829) remained unaffected by alkali metal ion loading. However, the new phases observed can be attributed to alkali metal oxides (Li_2O, K_2O, and Cs_2O) (JCPDS 9-355, 23-493, 26-1327, and 10-248); indeed, Cs-MgO was dominated by Cs_2O phase. Crystallite sizes calculated using Scherrer's equation [51] for all of the catalysts are given in Table 3. Nanocrystalline MgO is evident from the crystallite size of about 12 nm for all of the calcined catalysts except Cs-MgO, which had a size of 19 nm. Scanning electron microscopy results (not shown) clearly hinted that the particle size remained the same on MgO and alkali-loaded MgO. Surface area and pore volume

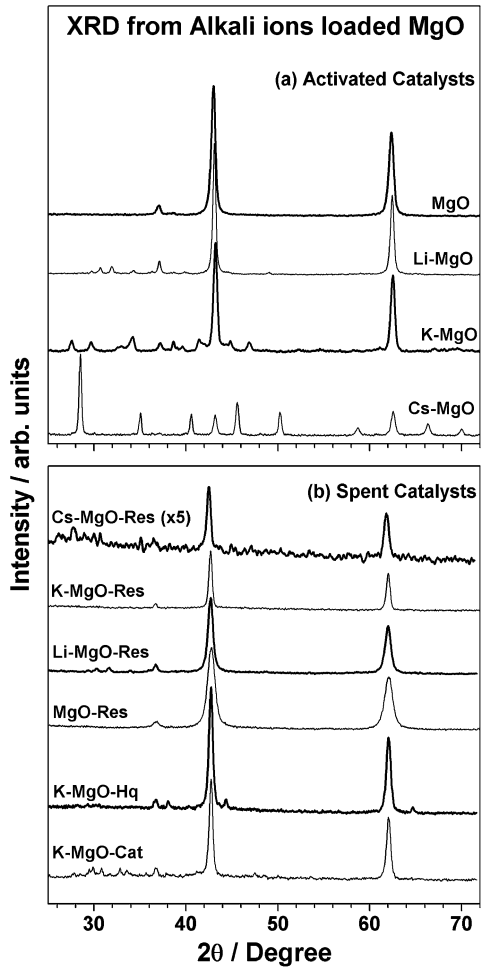

Fig. 10. XRD pattern from MgO and alkali metal ion-loaded MgO. (a) Activated catalysts (calcined at 673 K for 2 h) and (b) spent catalysts (after O-methylation of dihydroxybenzene carried out for 4 h TOS at 583 K).

(V_p) measured from N_2 sorption isotherms using BET method on alkali ion-loaded MgO decreased gradually with increasing alkali metal ion content and ionic radius, as shown in Table 3. The very low V_p on Cs-MgO suggests effective pore filling and hence rapidly declining catalytic activity for all DHB substrates.

XRD of representative spent catalysts after reaction for 4 h on stream (Fig. 10b) showed no new reflections, whereas the intensity of reflections due to alkali metal oxides (Li_2O, K_2O, and Cs_2O) decreased or disappeared after the reaction. Further, the broad features observed for spent catalysts compared with the sharp and intense features on calcined (MgO, Li-MgO, and Cs-MgO) catalysts indicate a decrease in crystallinity and crystallite size; this was marginal (severe) in the case of K-MgO (Cs-MgO and MgO) (Table 3). Surface area also decreased for spent catalysts, indicating the presence of significant carbonaceous products on the catalyst surface. The percentage drop in surface area after reaction was lower for K-MgO (14–36%) than for any other catalyst. In fact, catechol and hydroquinone methylation on K-MgO hardly deactivated, and the aforementioned decrease in surface area hardly affected the performance.

Table 3
Physical and textural properties of activated and spent MgO and alkali metal ion-loaded MgO catalysts

Catalysts	Crystallite size (nm); spent (activated)	BET surface area (m^2/g); spent (activated)	Pore volume activated (10^{-2} cc/g)
MgO-Res	6.5 (11.8)	21 (60)	13
Li-MgO-Res	8.4 (12.6)	24 (49)	11
K-MgO-Res	10.6 (11.8)	18 (28)	3
Cs-MgO-Res	10.1 (19.3)	6 (16)	1
K-MgO-Cat	11 (11.8)	24 (28)	–
K-MgO-Hq	11.5 (11.8)	21 (28)	–

3.5. Thermal analysis

Figs. 11a–11c show TG and derivate TG (DTG) profiles from spent K-MgO in air atmosphere after catechol, resorcinol, and hydroquinone methylation for 1 h at 583 K. The initial weight loss (<10%) observed at around 400 K on all of the spent catalysts is attributed to the loss of water. A large amount of carbon deposition is evident from the weight loss observed between 420 and 750 K in the TGA profiles. The total percent weight loss observed at 1000 K was about 40% with catechol, 60% with resorcinol, and 50% with hydroquinone spent catalysts. For catechol and resorcinol, the DTG showed two-stage weight losses at 575–645 K and 670–740 K, respectively; with hydroquinone, one major weight loss at 640 K and a minor loss at 710 K were observed. The weight loss at 740 and 710 K shown in Figs. 11b and 11c, respectively, may be due to the presence of high boiling biphenolic compounds. The presence of these compounds was indicated in the GC–MS analysis of resorcinol methylation products.

Fig. 11d shows the differential thermal analysis (DTA) traces in which a positive microvolt (μV) heat flow at respective temperatures was observed due to carbon burning in air atmosphere. This demonstrates that the observed TG weight losses are exothermic in nature, as expected. Further, the peak at 640–670 K in all three cases is interesting, hinting at the similar nature of the carbon deposits, which is likely polyaromatics [45,46].

Adsorbed molecular components, such as reactants and products, will become oxidized in air; thus, it is difficult to account for the weight losses by carrying out thermal analysis only in air atmosphere. However, thermal analysis in N_2 atmosphere might reveal (to a limited extent) the nature of the desorbing components. Figs. 11e, 11f, and 11g (thick traces) show the TG results carried out in N_2 atmosphere for K-MgO spent catalysts with all three DHB reactants. Note that the weight loss for catechol, resorcinol, and hydroquinone is approximately 40% at 1473 K, in contrast to the higher weight loss due to complete burning at 1000 K in air atmosphere for resorcinol and hydroquinone. Two broad weight losses were noted for all of the spent catalysts in the DTG profiles at 500–800 K and 1100–1300 K. DTA traces (Fig. 11h) show an endothermic weight loss processes, unlike that occurring in air atmosphere. In the case of catechol, these two weight losses were not very distinct, whereas resorcinol and hydroquinone

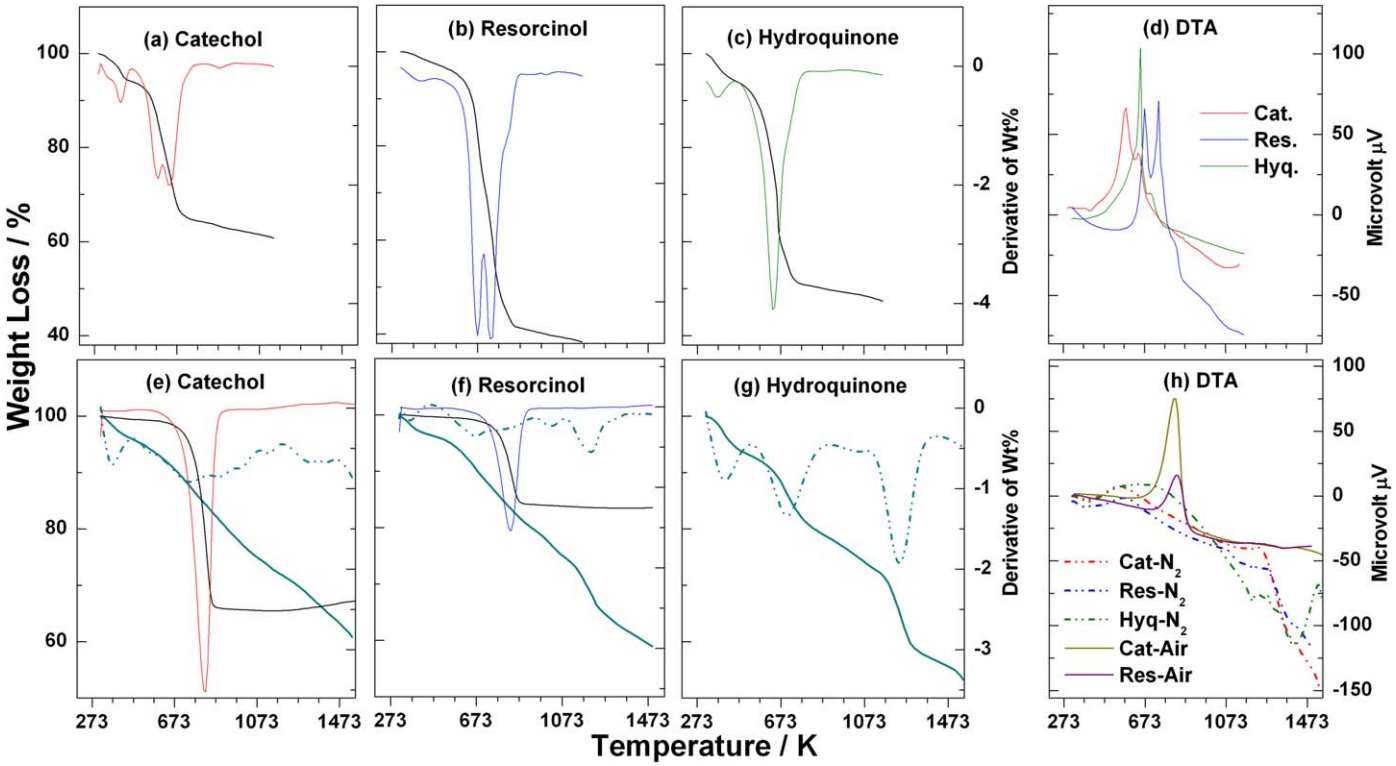

Fig. 11. Thermal analysis of K(5)-MgO spent catalyst after methylation of all three dihydroxybenzenes at 583 K, WHSV = 9.7 h^{-1} for 1 h with DMC:DHB = 2:1 feed mixture. TGA and derivative of TGA (DTG) weight loss under air (a–c) and N_2 (e–g) atmosphere with corresponding DTA in (d) and (h), respectively. TGA and DTG carried out subsequently in air atmosphere, after N_2 atmosphere analysis of catechol (e) and resorcinol (f) and corresponding DTA in (h).

showed sharp and distinct weight losses. The spent catalysts subjected to thermal analysis in N_2 atmosphere were subsequently subjected to thermal analysis in air atmosphere without being removed from the thermal analyzer; the results for catechol and resorcinol catalysts are shown in Figs. 11e and 11f (thin traces), respectively. Exothermic DTA profiles for these catalysts showed a single sharp peak (Fig. 11h) at around 830 K, again indicating a similar nature of carbon, which is likely to be polyaromatic, because it cannot be oxidized/desorbed in nitrogen.

3.6. ^{13}C CP-MAS NMR

Fig. 12 shows ^{13}C CP-MAS NMR results from spent K-MgO catalysts after catechol and resorcinol methylation reaction at 583 K for 1 h. Peaks related to adsorbed reactants and/or products (112 ppm), carbons without protons but attached to heteroatom (152 ppm), alkyl groups/chains (20 ppm), $MgCO_3$ (170 ppm), and polyaromatics (125 ppm) were identified from the different broad features. Clearly, the spectral feature was strongly dominated by aromatic species [52]. The strong peak at 125 ppm can be attributed to polyaromatic species due to polymerization of reactant/product molecule in different environment. This was the main species blocking the active sites. In the case of catechol, this strong peak appeared very sharp and symmetrical; however, in resorcinol it was broad with shoulders from different carbon species mentioned above.

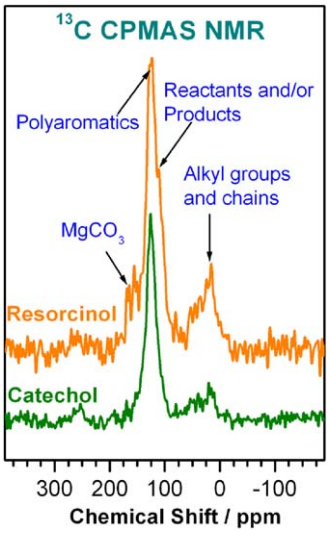

Fig. 12. ^{13}C CP-MAS NMR spectra from K(5)-MgO spent catalyst after catechol/resorcinol O-methylation at 583 K, WHSV = 9.7 h^{-1} for TOS = 1 h with DMC:dihydroxybenzene = 2:1 feed mixture.

Alkyl carbon species was also observed (20 ppm) on both catalysts, indicating the presence of methylated products or alkyl chains/groups. The alkyl feature was relatively broad and strong for resorcinol catalyst. It is worth correlating the lower-intensity alkyl feature and more effective DMC utilization of catechol case (Fig. 2) compared with resorcinol (Fig. 6). Carbonate carbon species, likely from $MgCO_3$ [53], was also ob-

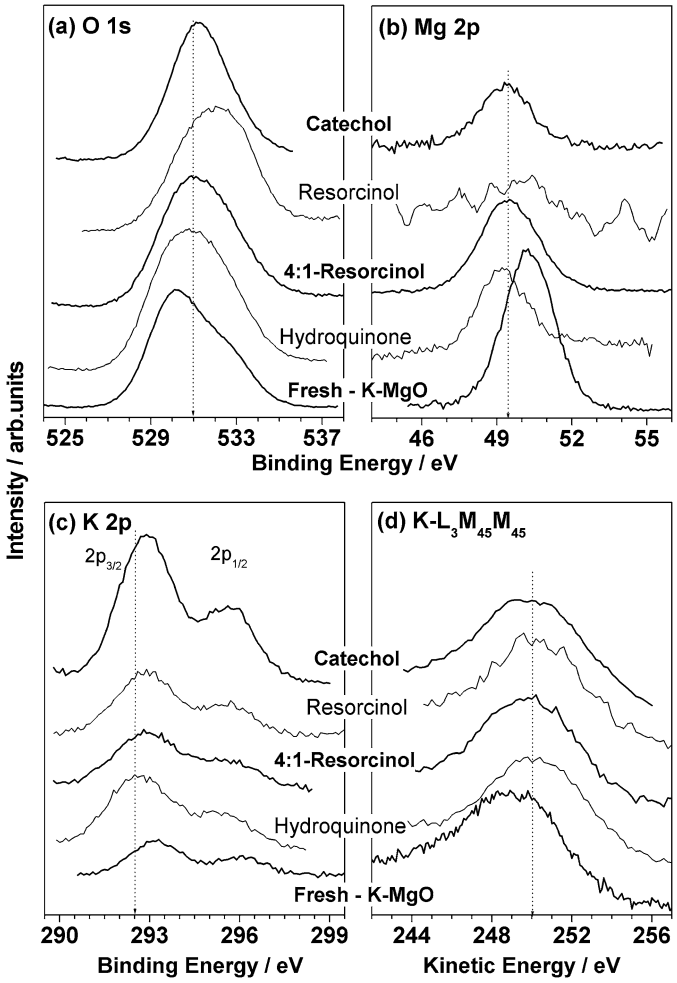

Fig. 13. X-ray photoemission spectra from K(5)-MgO spent catalysts after O-methylation of dihydroxybenzenes at 583 K and at WHSV = 9.7 h^{-1} for 1 h on TOS with DMC:DHB = 2:1 feed mixture. XPS results from fresh K(5)-MgO is also given for comparison. Dotted lines are guide to the eye.

served at 168 ppm in the resorcinol catalyst. Indeed, more $MgCO_3$ was evident on resorcinol from the relatively high weight loss at around 1000 K than in catechol, which showed only marginal weight loss (Figs. 11e–11f).

3.7. XPS analysis

3.7.1. O 1s, Mg 2p, C 1s, and K 2p core-level analysis

Fig. 13a shows O 1s spectra from K-MgO spent and calcined catalysts. The O 1s spectrum was very broad for the calcined catalyst, with a main peak centered at 530.2 eV and a shoulder at 532.3 eV attributed to the hydroxyl groups from adsorbed moisture on the catalysts [54]. Spent K-MgO catalysts showed a sharp peak at 531 eV after a 1-h methylation test. A shift in BE of around 1.8 eV (532 eV) was observed only on resorcinol (DMC:resorcinol = 2:1 feed). This indicates an onset in change in surface characteristics toward deactivation in resorcinol (Fig. 5). Fig. 13b shows Mg 2p spectra from calcined and spent K-MgO catalysts. A sharp peak at 50.3 eV was observed for the calcined sample, as is typical for Mg^{2+}. However, the Mg 2p intensity observed at 49.4 eV was low on all of the spent catalysts. Very poor or no Mg 2p intensity on resorcinol (DMC:resorcinol = 2:1) can be attributed to poor surface Mg^{2+} concentration.

Table 4
Surface atomic ratio of K-MgO fresh and spent catalysts

Atomic ratio	Fresh catalyst	Spent catalyst[a]			
		Catechol	Resorcinol	4:1, DMC:Res	Hydroquinone
K/Mg	0.024	2.565	2.153	0.017	0.147
K/C	–	0.478	0.055	0.078	0.086
Mg/C	–	0.186	0.025	4.690	0.582
(K + Mg)/C	–	0.665	0.080	4.769	0.667

[a] K/MgO catalyst was subjected with all reactants at optimum reaction conditions (space velocity = 6 h^{-1}; reaction temperature = 583 K; TOS = 1 h). 2:1 ratio of DMC:DHB was employed for all cases and 4:1 ratio was employed additionally with resorcinol.

Figs. 13c and 13d show K 2p and K-$L_3M_{45}M_{45}$ Auger electron emission, respectively, from calcined and spent K-MgO catalysts. The calcined sample exhibited two peaks at 293.3 and 296 eV, attributed to K $2p_{3/2}$ and $2p_{1/2}$, respectively. The spent samples showed similar features at lower BEs, at 292.8 and 295.5 eV. The higher K 2p intensity on all of the spent catalysts compared with the calcined catalyst is interesting, hinting at significant surface modification and altered surface composition due to reaction. This difference between calcined and spent catalysts in K 2p level was also well reflected in the Auger spectral results. The K-$L_3M_{45}M_{45}$ level appeared at 249 eV for the calcined catalyst, compared with 250 eV for the spent catalysts.

3.7.2. Surface composition

Table 4 gives the surface atomic ratios of calcined and spent K-MgO catalysts. It is evident from the Mg/C and K/Mg ratios that surface Mg content decreased during reaction. Very low Mg/C was observed after reaction with 2:1, DMC:resorcinol. However, reaction with 4:1, DMC:resorcinol feed had a greater amount of surface Mg, as evident from the very low K/Mg (0.017) and very high Mg/C (4.769) ratios. Surface K concentration was high for the spent catalysts compared with the calcined catalyst, except for 4:1, DMC:resorcinol reaction, as evident from the K/Mg ratio. Comparable K/C ratios were found for all of the spent catalysts, except for a very high K/C after the catechol reaction, indicating the surface was enriched with K. (K + Mg)/C showed very high (low) carbon content after 2:1 (4:1), DMC:resorcinol reaction, indicating a drastic change in surface composition, depending on the DMC content in the reaction. Catechol and hydroquinone catalysts showed comparable (K + Mg)/C ratios.

4. Discussion

4.1. O-methylation of DHBs on alkali ion-loaded MgO

Selective 2-MP production from catechol on MgO and 5 mmol alkali ion (Li, K, or Cs)-loaded MgO was carried out with DMC; only K-MgO showed stable activity. Secondary products like PCC, 1,2-DMB, and C-methylated catechol formation competed with each other depending on the reaction

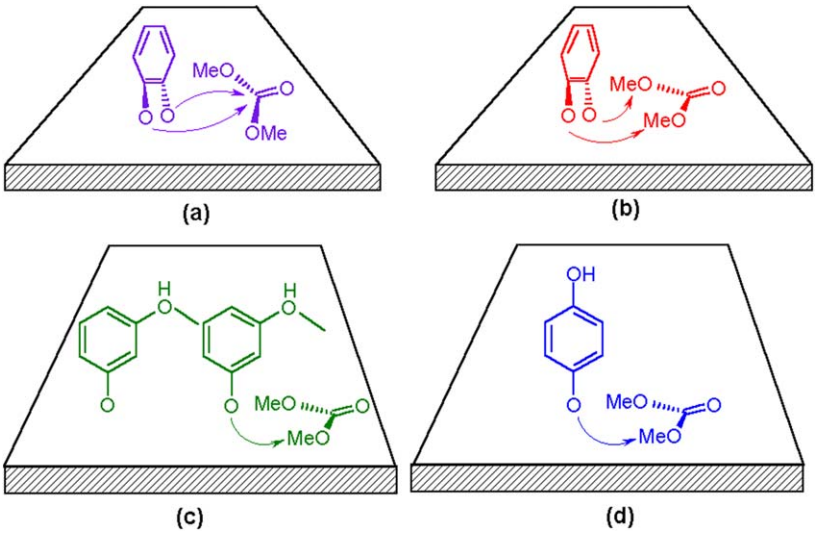

Fig. 14. Pictorial representation of (a) catechol carbonate and (b) 1,2-dimethoxybenzene formation from catechol. O-methylation and intermolecular interactions on (c) resorcinol and (d) hydroquinone.

conditions. PCC formation increased with TOS on all of the systems except K-MgO, in which a sizeable amount of 1,2-DMB formed. In general, 2-MP selectivity (70–80%) was not significantly affected by side products, catalysts, and reaction conditions, with the exception of a higher DMC:catechol (4) ratio. However, 1,2-DMB formation through PCC methylation was confirmed by temperature-dependent and WHSV-dependent studies. Thus, a sequential methylation step of 2-MP to 1,2-DMB may either be ruled out or may have occurred at a minimum level. The mono to di O-methylation ratio of >1 and the stable 2-MP selectivity of 70–75% at space velocity $<14.5\ h^{-1}$ indicated no sequential methylation of 2-MP to 1,2-DMB. A linear increase in O-methylation capacity with K concentration and very low levels of side products at high space velocity ($\geqslant 14.5\ h^{-1}$) clearly hinted that optimizing the process conditions with selective removal of 2-MP could lead to the selective production of 2-MP.

Similarity between the hydroquinone and catechol cases is evident by the selective formation of methoxy phenols on K-MgO with very low levels of side products at high WHSV ($\geqslant 14.5\ h^{-1}$). In contrast, $\geqslant$90% 4-MP selectivity at all WHSV values indicated a perfect perpendicular orientation of the hydroquinone aromatic ring to the catalyst surface. Significant formation of 1,4-DMB occurred at DMC:hydroquinone = 4 at the cost of 4-MP, indicating sequential methylation; however, isomerization of methylated hydroquinone to 1,4-DMB cannot be ruled out. Indeed, $\geqslant$95% 1,2-DMB selectivity observed at DMC:catechol = 4 supports the parallel orientation of catechol on the catalyst surface (Fig. 14b).

Unlike catechol or hydroquinone methylation, resorcinol methylation activity declined rapidly on all of the catalyst systems, due to resorcinol condensation producing polyphenolic chains that block the active sites, as shown in NMR and thermal analysis. However, K-MgO showed relatively better activity among the systems studied. Further, stable resorcinol conversion was observed with increasing amounts of DMC, due to prevention of the intermolecular interaction of resorcinol on the catalyst surface. Note that C-methylated product formation was significant on all of the catalyst systems except Cs-MgO, indicating that moderate-strength basic sites may be responsible for aromatic ring methylation. Indeed, the same trend was observed with catechol and hydroquinone. The maximum and stable O-methylation activity for all three DHB substrates observed on K-MgO compared with other systems indicates that an optimum basicity is required, not high (Cs-MgO) or low basicity (MgO and Li-MgO).

3-MP selectivity in resorcinol methylation was mainly affected by sequential methylation to 1,3-DMB. Note that whenever the resorcinol conversion increased, a simultaneous increase in 1,3-DMB was also observed. Even with high DMC content and stable resorcinol conversion on K-MgO at 583 K, a large 1,3-DMB selectivity (75%) was observed during initial TOS (Fig. 6c). Thus, it is clear that in the transient state at $\geqslant$563 K, sequential methylation of 3-MP to 1,3-DMB occurred. 3-MP selectivity increased to a greater extent at higher TOS as well as at higher space velocity ($\geqslant 18\ h^{-1}$), as evident from the mono to di O-methylation ratio shown in Fig. 7b. The foregoing findings indicate that a change in the catalyst surface occurred in the first few hours on stream and reached a state at which stable activity was observed, meriting further investigation.

4.2. Reactivity of DHBs

Reaction results suggest that although the three DHB compounds are just isomers, they have significantly different reactivities. The variation in reactivity trends is due mainly to differences in acidity. The acidities of these three compounds are in the following order: catechol < hydroquinone < resorcinol. Because MgO and alkali metal ion-loaded MgO are basic catalysts, most acidic resorcinol chemisorbs strongly and deactivates the active basic sites, which does not occur with other two isomers. This finding is supported by the highest carbon content observed in thermal analysis on spent catalyst from resorcinol.

The probability of the hydroxyl groups reacting toward catalyst surfaces drives the product selectivity. For instance, catechol has a high likelihood of both hydroxyl groups interacting on the catalyst surfaces, as shown in Figs. 14a and 14b. Thus, the formation of PCC and 1,2-DMB would be expected, as was indeed observed. In general, 1,2-DMB formation is likely through any of three possible routes: direct O,O-dimethylation of catechol, PCC ring opening followed by dimethylation, and methylation of 2-MP. 1,2-DMB formation through sequential methylation of 2-MP was already ruled out. Temperature-dependent studies of product selectivity have shown that 1,2-DMB forms only at the expense of PCC. An exception is direct O,O-dimethylation of catechol to 1,2-DMB, which likely is possible when excess DMC is available in the feed (Fig. 14b).

In resorcinol and hydroquinone, only one of the hydroxyl groups interacted with the catalysts surfaces. Thus, the interacting hydroxyl group was becoming methylated, and the selectivity for MPs was quite high. However, the free hydroxyl group likely facilitated an intermolecular interaction between resorcinol molecules, leading to polyaromatic chain formation (Fig. 14c). The spatial arrangement of OH groups in resorcinol and its acidity enhanced the condensation process. In hydroquinone (Fig. 14d), the free OH group spatial arrangement was such that it could condense with another gas-phase molecule; however, the stable activity suggests that this condensation was unlikely. Thus, no extensive polyaromatic chain formation with hydroquinone was observed, as evident from thermal analysis and catalytic activity.

4.3. Physicochemical and spectroscopic analysis

XRD of spent catalysts revealed that reaction conditions led to a significant breakup of crystallites on MgO, Cs-MgO, and especially Li-MgO. Thus, heavy carbon deposition on the catalyst surfaces buried the active centers completely and rapidly, leading to faster deactivation on the above catalyst systems. Surface area analysis of spent catalysts also supports the above conclusions. In contrast, marginal changes in the crystallite size and surface area of K-MgO show its robustness to reaction conditions and hence stable activity.

Thermal analysis in N_2 atmosphere revealed the presence of adsorbed reactants and/or products along with polyaromatics, as evident from the low-temperature (below 1000 K) weight loss peak. The minor weight loss observed at 580 K in air atmosphere and the broad weight loss observed at 500–850 K in N_2 atmosphere in catechol and its optimum reaction temperature at 583 K supports that the above carbon species are from adsorbed molecular components. Similar molecular component desorption in N_2 atmosphere was seen in hydroquinone (at 570–850 K) and resorcinol (at 573–1000 K). The high temperature (740 K) of the second weight loss peak in resorcinol suggests the strong chemisorption of resorcinol. ^{13}C CP-MAS NMR results obtained on the spent catalysts exhibiting chemical shifts characteristic of different carbon species were in good agreement with thermal analyses. Chemical shifts relating to carbonate carbon on $MgCO_3$ indicated the interaction between MgO and CO_2 or DMC directly.

Partial decomposition of polyaromatics to hydrogen-deficient polyaromatics or graphitic carbon during thermal analysis in N_2 atmosphere is evident from the successive weight loss at 850 K during air atmosphere analysis of the same sample. It is evident from the weight loss [resorcinol (63%) > hydroquinone (50%) > catechol (40%)] that the most acidic resorcinol made the highest molecular mass polyaromatic chains, followed by hydroquinone and catechol. Condensation or polymerization of the acidic reactants was boosted by the basic sites of the catalysts.

XPS reflects the changes on the catalysts due to reaction through changes in BE and surface atomic composition. The O^{2-} ions on the surface of spent catalysts have an electronic interaction with DHB protons and hence a shift in the BE of O 1s core level was observed compared with calcined catalyst. Resorcinol, having the most acidic protons, interacted very strongly, producing a large shift in O 1s BE. The increasing O 1s BE from 530.2 eV indicates that the basicity of the surface decreased during methylation, to a large extent for resorcinol. Thus, the descending basicity led to the deactivation with TOS during resorcinol methylation.

Mg 2p core level appeared at a lower BE (by 1 eV) on spent catalysts compared with fresh catalyst. It is likely that dissociative adsorption of DHB as hydroxy phenolate anions and protons occurred on the catalyst surface; the former made the Mg sites electron-rich. The decreasing Mg 2p spectral intensity on spent catalyst indicates that the surface Mg^{2+} species was buried under the deposited carbon species. The absence of Mg 2p core-level emissions in resorcinol (DMC:resorcinol = 2) reveals a severe coke deposition and hence a burial of Mg into the bulk. Indeed, Cs-MgO-Res showed no Cs_2O phase on XRD, supporting the significant coke deposition. The very low surface Mg content on K-MgO-Res (2:1) catalyst changed dramatically to very high when using excess DMC (K-MgO-Res—4:1), because excess DMC in the feed hindered effective intermolecular interaction, as suggested earlier. This also confirms the need for basic MgO support for the reaction.

The K 2p core level observed at lower BE than that of fresh catalyst is also reflected in the K-$L_3M_{45}M_{45}$ Auger transition appearing at higher kinetic energy. This shift in the binding and kinetic energies are due to the interaction of hydroxy phenolate anions with the K site. The high K content on spent catalyst surfaces compared with that on fresh K-MgO indicates significant surface segregation of K due to reaction at >583 K.

5. Conclusion

A comprehensive study on O-methylation of DHBs with DMC was carried out on MgO and alkali metal ion (Li, K, and Cs)-loaded MgO under vapor-phase conditions. Pure MgO had O-methylation activity that declined rapidly with time on stream. Alkali metal ion-loaded MgO showed better activity than pure MgO with all substrates. Among the catalyst systems screened, K-MgO showed the best mono O-methylation activity with relatively high stability for all substrates, hinting at the optimum basicity requirement. Reactivity and product selectivity were influenced by substrate acidity and mode of in-

teraction on the catalyst surfaces. Catechol interacting through 1,2 hydroxyl groups on the catalyst surfaces gave more secondary products, including PCC and veratrole; however, 2-MP selectivity possibly can be further maximized by varying the reaction conditions. Resorcinol and hydroquinone interactions left one hydroxyl group free in the space, and this free spatial hydroxyl group aided polyaromatic chain formation and blocked the active sites leading to catalyst deactivation with TOS. Low temperature (<610 K) led to high selectivity for MPs compared with the dimethoxybenzene selectivity reported in the literature. Large amounts of carbon deposits, as detected by thermal analysis, shed light on the mechanisms behind this catalyst deactivation. ^{13}C NMR revealed the presence of heavier polyaromatics and surface carbonates on spent catalysts. The surface basicity decreased during DHB interaction, as shown by XPS studies, and the significant basicity loss led to faster deactivation in the case of resorcinol methylation.

Acknowledgments

The authors thank the reviewers for many helpful suggestions for improving the manuscript. They also thank Drs. P.R. Rajmohanan, T.G. Ajithkumar, P.A. Joy, and S. Mayadevi for helpful discussions on the NMR and thermal analysis results. M.V. thanks CSIR, New Delhi for a research fellowship.

References

[1] T. Kotanigawa, M. Yamamoto, K. Shimokawa, Y. Yoshida, Bull. Chem. Soc. Jpn. 44 (1971) 1961.
[2] T. Kotanigawa, K. Shimokawa, Bull. Chem. Soc. Jpn. 47 (1974) 1535.
[3] K. Tanabe, H. Hattori, T. Sumiyoshi, K. Tamaru, T. Kondo, J. Catal. 53 (1978) 1.
[4] H. Grabowska, W. Kaczmarczyk, J. Wrzyszcz, Appl. Catal. 49 (1989) 351.
[5] H. Grabowska, W. Mista, L. Syper, J. Wrzyszcz, M. Zawadski, J. Catal. 160 (1996) 134.
[6] H. Grabowska, W. Mista, L. Syper, J. Wrzyszcz, M. Zawadski, Appl. Catal. 144 (1996) L1.
[7] H. Grabowska, W. Mista, L. Syper, J. Wrzyszcz, M. Zawadski, Angew. Chem. Int. Ed. Engl. 35 (1996) 1562.
[8] H. Grabowska, W. Mista, J. Trawczynski, J. Wrzyszcz, M. Zawadski, Appl. Catal. A Gen. 220 (2001) 207.
[9] H. Grabowska, R. Klimkiewicz, W. Tylus, P.J. Godowski, Appl. Catal. A Gen. 240 (2003) 111.
[10] E. Santacesaria, D. Grasso, S. Carra, Appl. Catal. 64 (1990) 83.
[11] V. Durgakumari, S. Narayanan, J. Mol. Catal. 65 (1991) 385;
V. Durgakumari, G. Sreekanth, S. Narayanan, Res. Chem. Intermed. 14 (1990) 223.
[12] A. Vinu, M. Karthik, M. Miyahara, M. Murugesan, K. Ariga, J. Mol. Catal. 230 (2005) 155.
[13] S. Velu, C.S. Swamy, Appl. Catal. A Gen. 119 (1994) 241.
[14] S. Velu, C.S. Swamy, Appl. Catal. A Gen. 145 (1996) 141.
[15] S. Velu, C.S. Swamy, Appl. Catal. A Gen. 162 (1997) 81.
[16] W.C. Choi, J.S. Kim, T.H. Lee, S.I. Woo, Catal. Today 63 (2000) 229.
[17] T. Tsai, F. Wang, Catal. Lett. 73 (2001) 167.
[18] T.M. Jyothi, T. Raja, M.B. Talawar, B.S. Rao, Appl. Catal. A Gen. 211 (2001) 41.
[19] T. Mathew, N.R. Shiju, K. Sreekumar, B.S. Rao, C.S. Gopinath, J. Catal. 210 (2002) 405;
T. Mathew, N.R. Shiju, V.V. Bokade, B.S. Rao, C.S. Gopinath, Catal. Lett. 94 (2004) 223.
[20] T. Mathew, S. Sylesh, B.M. Devassy, M. Vijayaraj, C.V.V. Sathyanarayana, B.S. Rao, C.S. Gopinath, Appl. Catal. A Gen. 273 (2004) 35.
[21] T. Mathew, M. Vijayaraj, S. Pai, B.B. Tope, B.S. Rao, S.G. Hegde, C.S. Gopinath, J. Catal. 227 (2004) 175.
[22] R. Bal, S. Sivasanker, Appl. Catal. A Gen. 246 (2003) 373.
[23] R. Bal, S. Sivasanker, Green Chem. 2 (2000) 106.
[24] R. Pierantozzi, A.F. Nordquist, Appl. Catal. 21 (1986) 263.
[25] M.C. Samolada, E. Grigoriadou, Z. Kiparissides, I.A. Vasalos, J. Catal. 152 (1995) 52.
[26] G. Sarala Devi, D. Giridhar, B.M. Reddy, J. Mol. Catal. A Chem. 181 (2002) 173.
[27] S. Balsama, P. Beltrame, P.L. Beltrame, P. Carniti, L. Forni, G. Zurelti, Appl. Catal. 13 (1984) 161.
[28] E. Santacesaria, M. Discrio, P. Ciambelli, D. Gelosa, S. Carra, Appl. Catal. 64 (1990) 101.
[29] V. Durgakumari, S. Narayanan, L. Guczi, Catal. Lett. 5 (1990) 377.
[30] Phenol Derivatives, in: Ullmann's Encyclopedia of Industrial Chemistry, vol. A19, VCH, Weinheim, 1991, p. 354.
[31] Y. Fu, T. Baba, Y. Ono, Appl. Catal. A Gen. 166 (1998) 419.
[32] Y. Fu, T. Baba, Y. Ono, Appl. Catal. A Gen. 166 (1998) 425.
[33] Y. Fu, T. Baba, Y. Ono, Appl. Catal. A Gen. 176 (1998) 201.
[34] Y. Fu, T. Baba, Y. Ono, Appl. Catal. A Gen. 178 (1999) 219.
[35] L. Calzolari, F. Cavani, T. Monti, Solid State Chem. Catal. 3 (2000) 533.
[36] F. Cavani, T. Monti, Catal. Org. Reactions 82 (2001) 123.
[37] F. Cavani, T. Monti, D. Paoli, Stud. Surf. Sci. Catal. 130 (2000) 2633.
[38] V. Vishwanathan, S. Ndou, L. Sikhwivhilu, N. Plint, K. Vijayaraghavan, N.J. Coville, Chem. Commun. (2001) 893.
[39] M.B. Talawar, T.M. Jyothi, P.D. Sawant, T. Raja, B.S. Rao, Green Chem. 2 (2000) 266.
[40] T.M. Jyothi, T. Raja, M.B. Talawar, B.S. Rao, Appl. Catal. A Gen. 211 (2001) 41.
[41] L. Kiwi-Minsker, S. Porchet, R. Doepper, A. Renken, Stud. Surf. Sci. Catal. 108 (1999) 149.
[42] L. Kiwi-Minsker, G. Jenzer, L. Pliasova, A. Renken, Stud. Surf. Sci. Catal. 121 (1999) 159.
[43] R. Bal, B.B. Tope, S. Sivasanker, J. Mol. Catal. A Chem. 181 (2002) 161.
[44] R. Bal, S. Mayadevi, S. Sivasanker, Org. Process Res. Dev. 7 (2003) 17.
[45] X. Zhu, X. Li, M. Jia, G. Liu, W. Zhang, D. Jiang, Appl. Catal. A Gen. 282 (2005) 155.
[46] Z. Fu, Y.Y.D. Yin, Y. Xu, H. Liu, H. Liao, Q. Xu, F. Tan, J. Wang, J. Mol. Catal. A Chem. 232 (2005) 69.
[47] S.B. Waghmode, R. Vetrivel, S.G. Hegde, C.S. Gopinath, S. Sivasanker, J. Phys. Chem. B 107 (2003) 8517.
[48] V.K. Diez, C.R. Apesteguia, J.I. Di Cosimo, J. Catal. 240 (2006) 235.
[49] T. Mathew, B.S. Rao, C.S. Gopinath, J. Catal. 222 (2004) 107.
[50] M. Vijayaraj, C.S. Gopinath, J. Catal. 241 (2006) 83.
[51] N.F.M. Henry, J. Lipsons, W.A. Wooster, The Interpretation of X-Ray Diffraction Photographs, Macmillan, London, 1951.
[52] The Aldrich Library of ^{13}C and ^{1}H FT NMR Spectra, vol. 2, first ed., Aldrich Chemical Co., Inc., Milwaukee, 1993.
[53] H.W. Papenguth, R.J. Kirkpatrick, B. Montez, P.A. Sandberg, Am. Mineral. 74 (1989) 1152.
[54] A. Miyakoshi, A. Ueno, M. Ichikawa, Appl. Catal. A Gen. 219 (2001) 249.